

Kinetics of the SiH₃ + H₂O₂ and SiH₃ + O₂ Reactions

Justin P. Meyer and John F. Hershberger*

Department of Chemistry, North Dakota State University, Fargo, North Dakota 58105

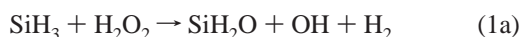
Received: October 21, 2002; In Final Form: May 12, 2003

The kinetics of the reaction of silyl radicals (SiH₃) with H₂O₂ and O₂ were studied using time-resolved infrared diode laser absorption spectroscopy. The rate constant SiH₃ + H₂O₂ at 298 K was determined to be $9.8 \times 10^{-12} \text{ cm}^3 \text{ molecule}^{-1} \text{ s}^{-1}$. This rate constant is independent of temperature over the range 298–573 K. The yield of OH products was quantified by reaction with CO to produce CO₂, which was detected by infrared spectroscopy. The branching ratio of the SiH₃ + H₂O₂ reaction into OH product channels was estimated to be <0.05 at 298 K. Similar experiments on the SiH₃ + O₂ reaction indicated an OH product branching ratio of 0.076 ± 0.04 at 298 K.

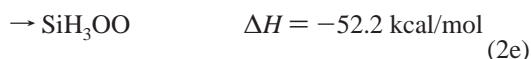
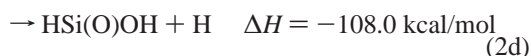
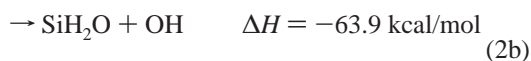
1. Introduction

The kinetics of main group hydride radicals are of interest in the modeling of chemical vapor deposition (CVD) processes for the fabrication of electronic and photovoltaic devices,^{1–5} as well as silane combustion.^{6,7} The SiH₃ (silyl) radical is believed to be especially important in plasma-enhanced CVD techniques used to deposit thin films of amorphous hydrogenated silicon (a-Si:H).^{2–5} As a result, numerous studies of the kinetics of this species have been reported,⁸ with published rate constants for reactions of SiH₃ with O₂,^{9–12} NO,^{10,12–13} NO₂,¹² SiH₃,^{14,15} HBr,¹⁶ S₂Cl₂,¹⁷ and several unsaturated hydrocarbons.¹⁵ Recent studies of SiO₂ deposition under photo-CVD conditions included H₂O₂ as one of several possible oxidants.^{18,19} Most of the rate constants used in the kinetic model were based on published measurements; however, a major exception was the SiH₃ + H₂O₂ reaction, for which an estimated rate constant of $1.2 \times 10^{-10} \text{ cm}^3 \text{ molecule}^{-1} \text{ s}^{-1}$ was used.¹⁹ No direct measurements of the kinetics of this reaction have been previously reported.

The SiH₃ + H₂O₂ reaction has several possible product channels:



Similarly, the reaction of silyl radical with molecular oxygen has several possible product channels:



The thermochemical data was taken from the G2 ab initio calculations of Darling and Schlegel.²⁰ Several other (less likely)

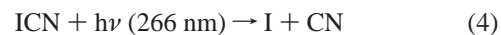
product channels were included in their calculations as well. They found a low energy pathway at the G2 level to product channel 2b, suggesting that OH radicals should be a major product in the reaction. Although the literature on total rate constants of reaction 2 is extensive, only one group has previously reported branching ratios. Koshi et al. used time-resolved LIF measurements of H and OH products to estimate $\phi_{2b} = 0.25 \pm 0.05$ and $\phi_{2c} = 0.65 \pm 0.05$ at room temperature.²¹ Darling and Schlegel suggested that the observed H atoms originated from secondary chemistry, such as OH + SiH₂O → HSi(O)OH + H.²⁰

We report here measurements of the total rate constant of reaction 1 over the temperature range 298–573 K using laser photolysis/infrared absorption spectroscopy. We also report an estimate for the 298 K branching ratio into the OH-producing channels of both reactions 1 and 2. The total rate constant of reaction 2 has been reported previously by several workers, and such measurements are not repeated here.

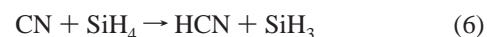
SiH₃ was produced in this study by reaction of photolytically generated Cl atoms or CN radicals with silane:



or



or



These reactions are fast, with $k_5 = (3.5–4.5) \times 10^{-10}$ and $k_6 = 2.4 \times 10^{-10} \text{ cm}^3 \text{ molecule}^{-1} \text{ s}^{-1}$ at 298 K.^{22–24} SiH₃ radicals formed in reactions 5 or 6 are detected by infrared laser absorption using a lead-salt diode laser at 2200–2230 cm⁻¹ corresponding to ⁴R branch transitions of the ν_3 stretching mode, which have been spectroscopically characterized.²⁵

2. Experimental

The time-resolved infrared diode laser technique has been described previously.^{11,26} Continuous, high resolution (0.0003 cm⁻¹) infrared radiation from a lead-salt diode laser (Laser

* To whom correspondence should be addressed.

Photonics) was made collinear with 266-nm radiation from an Nd:YAG laser (Lumonics) by means of a dichroic mirror. Both laser beams passed through a 6-mm iris in order to precisely define the beam diameter. The beams were then copropagated down a 1.43-m Pyrex absorption cell and passed through a second 6-mm iris. The infrared light then passed through a 0.25-m monochromator and was focused onto an InSb detector (Cincinnati Electronics, $\sim 1 \mu\text{s}$ response). Transient signals were collected and averaged on a digital oscilloscope and stored on a computer. The HITRAN database²⁷ and published spectral data²⁵ for SiH_3 were used as an aid in calibrating laser wavelengths and identifying transitions.

All experiments were performed on static gas mixtures. To ensure complete mixing of reagents, gases were allowed to stand for 5 min in the reaction cell. Typically, only 5–10 laser shots were signal averaged for both the total rate constant and product yield experiments. Under these conditions, only minimal build-up of products or depletion of reactants was observed.

SiH_4 (Matheson), SF_6 (Matheson), and S_2Cl_2 (Aldrich) were purified by freeze–pump–thaw cycles at 77 K. O_2 (Matheson, research grade) was used without further purification. ICN (Fluka) was purified by vacuum sublimation to remove dissolved air. H_2O_2 (Aldrich, 50% in H_2O) was purified by extensive pumping to remove the more volatile water component. After purification, the H_2O_2 solution was estimated to be 95 mol % pure for a vapor phase purity of $63 \pm 10\%$ H_2O_2 , $37 \pm 10\%$ H_2O , assuming Raoult's Law. Vapor phase H_2O_2 pressures reported here include this 0.63 correction factor. The SiH_3 radical does not react with H_2O , so the presence of H_2O does not severely affect these experiments.

3. Results

3.1. Total Rate Constants. Upon photolysis of ICN/ SiH_4 / SF_6 or S_2Cl_2 / SiH_4 / SF_6 mixtures, several transient absorptions attributed to SiH_3 radicals were found in the 2200–2230 cm^{-1} region, as predicted by spectroscopic studies. The $\text{R}_0(1)$ and $\text{R}_5(3)$ lines at 2201.82 and 2226.26 cm^{-1} , respectively, were chosen for kinetic studies, based on minimal overlap with SiH_4 lines and optimum probe laser intensity. Results obtained using these spectral lines were identical. Using typical photolysis laser energies of ~ 5 – 7 mJ/pulse, transient absorptions of $\sim 15\%$ of the probe laser intensity were observed. Small off-resonant background transients (5–20% of the on-resonant transient) were observed when the probe laser was detuned $\sim 0.02 \text{ cm}^{-1}$ off the SiH_3 line. These background signals, which are attributed to thermal deflection of the probe laser, were subtracted from the on-resonant signals to obtain SiH_3 time-resolved absorption profiles. A typical SiH_3 signal is shown in Figure 1. These signals display a fast, detector-limited rise followed by a slower decay, consistent with rapid SiH_3 production by reaction 5 or 6, followed by reaction of SiH_3 .

Typical reaction conditions were 0.025 Torr of S_2Cl_2 precursor, 0.3 Torr of SiH_4 , 0.0–0.4 Torr of H_2O_2 , and 0.5 Torr of SF_6 buffer gas. Under these conditions, and at our photolysis laser pulse energies, typical SiH_3 radical densities of $\sim 10^{13}$ molecule cm^{-3} (~ 0.3 mTorr) are obtained. Pseudo-first-order conditions of $[\text{SiH}_3] \ll [\text{H}_2\text{O}_2]$ were therefore met whenever H_2O_2 reagent was included. The SF_6 buffer gas was included because it is an efficient collisional relaxer of vibrational excitation of many small molecules. Except for somewhat smaller magnitude, identical results were obtained using ICN as the radical precursor.

The decay portions of the transient signals were fit to single exponential decays to obtain pseudo-first-order rate constants k' . Figure 2 shows a plot of pseudo-first order rate constant vs

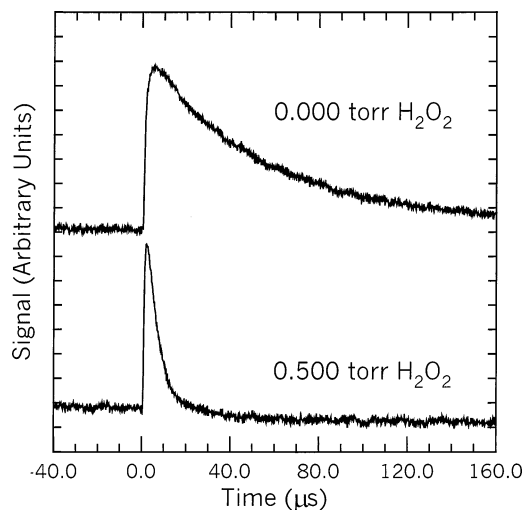


Figure 1. Transient infrared absorption signals of the SiH_3 radical at 2226.26 cm^{-1} . Reaction conditions: $P_{\text{S}_2\text{Cl}_2} = 0.025$ Torr, $P_{\text{SiH}_4} = 0.30$ Torr, $P_{\text{H}_2\text{O}_2} = 0.0$ Torr (top trace), 0.315 Torr (bottom trace), $P_{\text{SF}_6} = 0.500$ Torr. Each trace is the average of 6 laser shots.

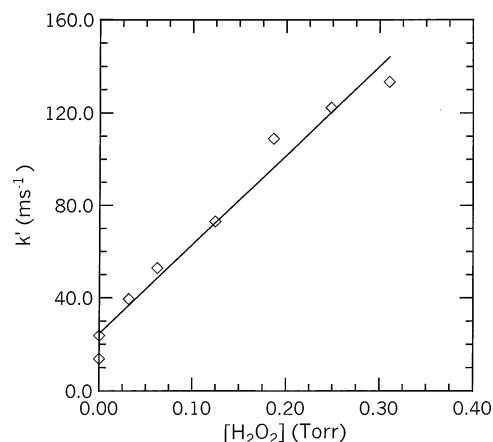


Figure 2. Pseudo-first-order decay rate constant of SiH_3 radical as a function of H_2O_2 pressure. Reaction conditions: $P_{\text{S}_2\text{Cl}_2} = 0.025$ Torr, $P_{\text{SiH}_4} = 0.30$, $P_{\text{H}_2\text{O}_2} = \text{variable}$, $P_{\text{SF}_6} = 0.500$ Torr.

H_2O_2 pressure. As per standard kinetic treatments, the slope of these plots gives the desired second-order rate constant k_1 . The nonzero intercept in Figure 2 is due primarily to the $\text{SiH}_3 + \text{S}_2\text{Cl}_2$ reaction, which has a rate constant of $(2.4 \pm 0.5) \times 10^{-11} \text{ cm}^3 \text{ molecule}^{-1} \text{ s}^{-1}$.¹⁷ Other (minor) contributions to the intercept include $\text{SiH}_3 + \text{SiH}_3$ self-reaction (or other radical–radical chemistry) and diffusion of SiH_3 out of the probed region in the cell. At the pressures and beam geometries used, diffusion occurs on a ~ 1 ms time scale, slower than the observed decays. Diffusion therefore does not significantly affect the transient signals. Because S_2Cl_2 is a viscous liquid with a fairly low vapor pressure, it is difficult to precisely control $[\text{S}_2\text{Cl}_2]$ in these experiments, so the reproducibility of the point at 0.0 Torr H_2O_2 is rather poor. When H_2O_2 reagent is included, most of the pseudo-first-order decay is due to the title reaction, and the reproducibility is better.

Experiments were conducted over the temperature range 298–573 K. Figure 3 shows an Arrhenius plot of the data. As shown, the rate constant is essentially independent of temperature over this range. The data were fit to the following Arrhenius expression (error bars represent one standard deviation):

$$k_1 = (9.7 \pm 1.8) \times 10^{-12} \exp[(3.2 \pm 61)/T] \text{ cm}^3 \text{ molecule}^{-1} \text{ s}^{-1}$$

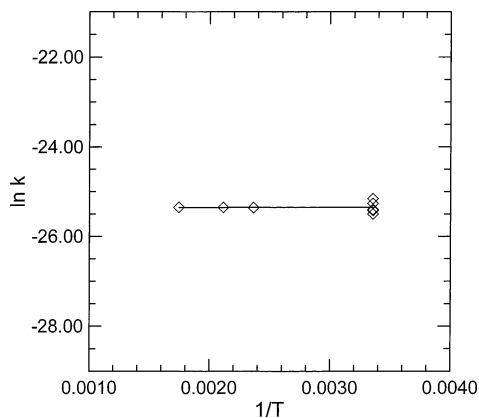


Figure 3. Arrhenius plot of the temperature dependence of the rate constant of the SiH₃ + H₂O₂ reaction.

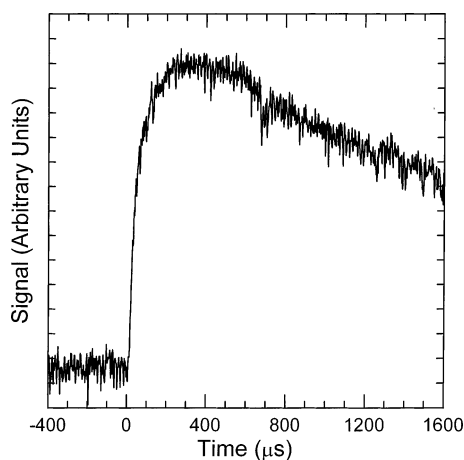
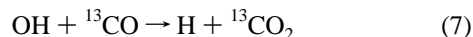


Figure 4. Transient signal (average of 6 laser shots) for ¹³CO₂ at 2308.172 cm⁻¹ produced in the SiH₃ + O₂ reaction, using ¹³CO to convert OH into ¹³CO₂ (see text). Reaction conditions: $P_{\text{ICN}} = 0.150$ Torr, $P_{\text{SiH}_4} = 0.025$ Torr, $P_{\text{O}_2} = 0.300$ Torr, $P_{\text{SF}_6} = 0.500$ Torr, $P_{\text{13CO}} = 7.35$ Torr.

3.2. Product Channels. No attempt was made to detect SiH₂O or SiH₃O, as there is no available spectroscopic information on these species. The OH radical formed in channel 1a or 2b is readily detectable by laser-induced fluorescence, but calibration of LIF signals to obtain absolute product yields can be difficult. The approach used here is to convert any OH radicals formed in 1a or 2b into CO₂ by reaction with an excess of CO. CO₂ is readily detected and quantified by infrared absorption spectroscopy:



This reaction has a low-pressure rate constant of $k_7 = 1.5 \times 10^{-13}$ cm³ molecule⁻¹ s⁻¹ at 298 K.²⁸ Carbon-13 labeled reagents were used because small amounts of CO₂ impurities in the reactants proved difficult to completely remove, resulting in significant static absorptions of ¹²CO₂ spectral lines. For detection, we chose the (00⁰) R(36) line of ¹³CO₂ at 2308.172 cm⁻¹. Figure 4 shows a typical transient signal for ¹³CO₂ upon photolysis of an ICN/SiH₄/O₂/¹³CO/SF₆ mixture. Similar looking transient signals were also obtained using an ICN/SiH₄/H₂O₂/¹³CO/SF₆ mixture. As shown, the signal has a rise time of ~150 μs, which is somewhat slower than would be predicted from the rate of reaction 7. We attribute this to the likely formation of vibrationally excited CO₂ molecules, which must be collisionally relaxed to the ground vibrational state. The inclusion of SF₆ buffer gas is primarily designed to accomplish

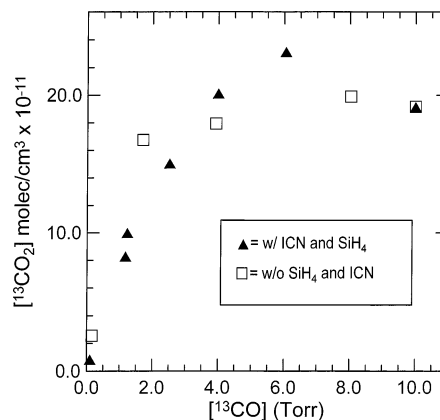


Figure 5. ¹³CO₂ product yield in the SiH₃ + H₂O₂ reaction, using ¹³CO to convert OH into ¹³CO₂ (see text). Data shown with (triangles) and without (squares) ICN/SiH₄ reactants. Reaction conditions: $P_{\text{ICN}} = 0.150$ Torr (triangles), 0.0 Torr (squares), $P_{\text{SiH}_4} = 0.05$ Torr (triangles), 0.0 Torr (squares), $P_{\text{H}_2\text{O}_2} = 0.190$ Torr, $P_{\text{SF}_6} = 0.500$ Torr, $P_{\text{13CO}} = \text{variable}$.

this vibrational relaxation. The slow decay, on a ~1–2 ms time scale, is due to diffusion of CO₂ out of the probed laser beam.

To quantify the [CO₂] yields, the slow decay portion of the transient ¹³CO₂ signals was fit to an exponential decay function. (Diffusion kinetics is not strictly exponential, but the approximation is sufficient for our purposes.) This function was extrapolated back to $t = 0$ to obtain the signal amplitude that would be expected if this decay were not present; this procedure resulted in values only slightly greater than peak-to-peak amplitudes. The amplitude was then converted into absolute number densities using equations described previously,²⁹ as well as tabulated linestrengths from the HITRAN database.²⁷ The only modification was that the linestrengths were corrected for isotopic enrichment by dividing by 0.011, which is the natural abundance value of ¹³C used in the database. Figure 5 shows the resulting ¹³CO₂ yield as a function of ¹³CO pressure for the SiH₃ + H₂O₂ reaction, with and without the ICN and SiH₄ reagents. (We prefer the use of ICN rather than S₂Cl₂ precursors in the product yield experiments, because the 266-nm absorption coefficient and photolysis quantum yield are better known for ICN.) The product yield in the absence of ICN and SiH₄ is attributed to formation of OH from direct photolysis of H₂O₂ at 266 nm. The ¹³CO₂ yield roughly levels off at high ¹³CO pressures, indicating that most OH radicals formed are converted into ¹³CO₂. When ICN and SiH₄ are included in the reaction, reactions 4 and 6 followed by 1a would be expected to produce additional OH radicals, resulting in an increased yield of ¹³CO₂. (Only a small pressure of SiH₄ is used in this experiment, to minimize competition between SiH₄ and CO for OH radicals). As shown, the product yields for H₂O₂/SF₆ and ICN/SiH₄/H₂O₂/SF₆ mixtures are virtually the same, indicating that essentially all of the observed product originated from H₂O₂ photolysis. Based on the uncertainties in the measurements, we estimate an upper limit of ~5 × 10¹¹ cm⁻³ for the number density of ¹³CO₂ produced by OH from reaction 1a. To obtain a branching ratio ϕ_{1a} , we calculate an initial CN radical density of 2.96 × 10¹³ cm⁻³ from the initial ICN pressure (0.15 Torr) and measurement of the photolysis laser pulse energy (6.1 mJ) and absorption coefficient of α (266 nm) = 0.0074 cm⁻¹ Torr⁻¹ for ICN and assuming a quantum yield for CN production of unity. The absorption coefficient was determined by measuring the fraction of 266 nm light transmitted through the cell with varying pressures of ICN. We also measured the magnitude of the SiH₃ transient signal vs SiH₄ pressure, as shown in Figure

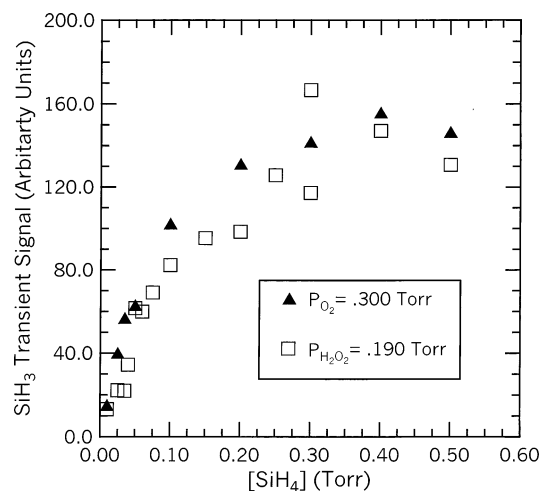


Figure 6. Peak magnitude of SiH₃ transient signal as a function of SiH₄ pressure. Reaction conditions: $P_{\text{ICN}} = 0.100$ Torr, $P_{\text{SiH}_4} = \text{variable}$, $P_{\text{H}_2\text{O}_2} = 0.190$ Torr (squares), 0.0 Torr (triangles), $P_{\text{O}_2} = 0.300$ Torr (triangles), 0.0 Torr (squares), $P_{\text{SF}_6} = 0.500$ Torr.

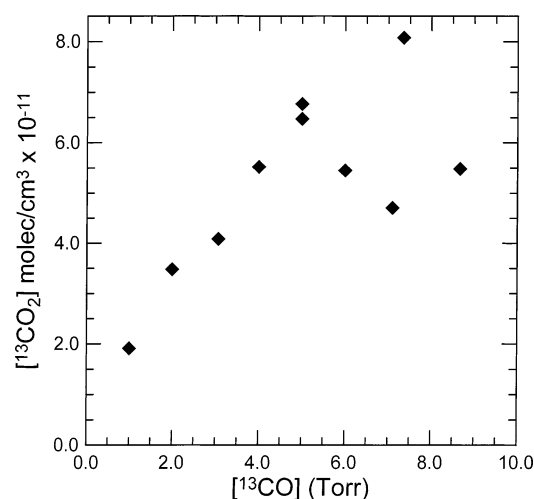


Figure 7. ¹³CO₂ product yield in the SiH₃ + O₂ reaction as a function of [¹³CO]. Reaction conditions: $P_{\text{ICN}} = 0.150$ Torr, $P_{\text{SiH}_4} = 0.025$ Torr, $P_{\text{O}_2} = 0.300$ Torr, $P_{\text{SF}_6} = 0.500$ Torr, $P_{\text{13CO}} = \text{variable}$.

6. This shows that at 0.05 Torr SiH₄ (the conditions used in Figure 5) only approximately 39% of the CN radicals have been converted into SiH₃. The remaining CN radicals are presumably removed by other paths, such as self-reaction, diffusion, reaction with CN + H₂O₂, etc. No literature data on the rate constant of CN with H₂O₂ are available, but it probably produces HCN + HO₂, which are not expected to affect these measurements. We then estimate that about 70% of the SiH₃ radicals reacted with H₂O₂, based on comparison of the intercept of Figure 2 with the k' value at 0.19 Torr H₂O₂ (the pressure used in the experiments of Figure 5). Using these numbers, we estimate an upper limit of the branching ratio $\phi_{1a} < 0.05$.

Similar OH yield experiments were performed for the SiH₃ + O₂ reaction. Figure 7 shows the resulting ¹³CO₂ yield as a function of ¹³CO pressure. In this reaction, there is no direct photolytic source of OH radicals, and the resulting signals are therefore attributed to reaction 2b followed by reaction 7. This assumption was verified by the observation that no ¹³CO₂ was formed upon photolysis of SiH₄/O₂/¹³CO/SF₆ mixtures, i.e., in the absence of the ICN precursor. From Figure 6, we estimate that, at 0.025 Torr SiH₄, about 27.5% of the CN radicals were converted into SiH₃. This is roughly consistent with the predicted relative rates of CN + O₂ and CN + SiH₄ under these

conditions. By a procedure similar to that described above for SiH₃ + H₂O₂, we estimate that about 84% of the SiH₃ radicals reacted with O₂ at $P_{\text{O}_2} = 0.300$ Torr. (Because we did not measure SiH₃ pseudo-first-order decay rates in the presence of O₂ in this study, we used our previous study of SiH₃ kinetics.)¹² After averaging several experiments of the type shown in Figure 7, we obtain a branching ratio of $\phi_{2b} = 0.076 \pm 0.04$ for the SiH₃ + O₂ reaction.

4. Discussion

Several possible secondary reactions could potentially affect the results. Because H₂O₂ samples, even purified, inevitably contain some water, we considered the SiH₃ + H₂O reaction. The decay rate of transient SiH₃ signals did not increase upon the addition of H₂O over the range 0–0.5 Torr, indicating that this reaction is extremely slow and does not affect the results for k_1 determination. We estimate an upper limit of 3×10^{-13} cm³ molecule⁻¹ s⁻¹ for the rate constant of SiH₃ + H₂O. The CN + H₂O reaction is very slow, with a measurable rate constant only above 500 K and a large activation energy.³⁰

If the radical density is high enough, radical–radical reactions such as SiH₃ + SiH₃, SiH₃ + CN, or reaction of SiH₃ with products of reaction 1 could contribute to the observed signal decay rates. These effects are minimized, however, by keeping radical densities as low as possible. Under our typical conditions using ICN precursor, about $\sim 10^{13}$ CN radicals cm⁻³ are initially formed. At these densities, a second-order radical–radical secondary reaction with a gas kinetic rate constant would occur with a half-life of ~ 500 μ s, which is far longer than the observed decay rates, even in the absence of added H₂O₂. Radical–radical chemistry therefore has an insignificant effect on the results.

Another potential complication is that H₂O₂ has a small but significant absorption coefficient at 266 nm, producing OH radicals. Using the high [CO] points in Figure 5, we estimate an OH yield from direct H₂O₂ photolysis of $\sim 2 \times 10^{12}$ cm⁻³. This density is roughly comparable to that calculated by using a measured crude estimate of $\alpha \sim 0.0005 \pm 0.0003$ cm⁻¹ Torr⁻¹ (base e) for H₂O₂ at 266 nm. Assuming a gas kinetic rate of 2×10^{-10} cm³ molecule⁻¹ s⁻¹ for the SiH₃ + OH reaction (probably an overestimate), we predict an SiH₃ lifetime of several milliseconds, an insignificant effect on the measured decay rates.

This work represents the first reported measurement of k_1 . The value obtained is significantly lower than the estimate used in the modeling study of photochemical SiO₂ deposition under H₂O₂ oxidant conditions.^{18,19} The extent to which this affects the model is not clear, as sensitivity analysis on the kinetic model was not performed. That model, however, considered SiH₂O formed in channel 1a to be the critical intermediate leading to film deposition. Because reaction 1a also forms OH radicals, which react with SiH₄, producing more SiH₃, this channel represents a chain branching step in the overall oxidation mechanism. Our experiments strongly indicate, however, that OH is at most a minor product of the SiH₃ + H₂O₂ and SiH₃ + O₂ reactions. This is a quite surprising result, especially for SiH₃ + O₂, for which previous work indicated $\phi_{2b} = 0.25$.²¹ Although secondary chemistry involving OH certainly occurs in this system, at the high CO pressures shown in Figures 5 and 7, OH removal should be dominated by reaction 7. For example, OH + SiH₄ has a rate constant of 1.2×10^{-11} cm³ molecule⁻¹ s⁻¹ at 298 K.³¹ Using 0.025 Torr SiH₄, the pseudo-first-order rates of OH removal by CO and SiH₄ are expected to become equal at 1.25 Torr CO, so that CO₂ formation from reaction 7 should be about half of the amount formed in the high [CO]

limit. This is in approximate agreement with the curve shown in Figure 7. At the highest CO pressures used, a small (~10%) fraction of OH radicals may still react with SiH₄, but this error is less than the quoted uncertainties in the branching ratios. It is thus very unlikely that we have severely underestimated the amount of OH in our experiments.

5. Conclusions

The reaction of SiH₃ with H₂O₂ was investigated. The total rate constant is $9.8 \times 10^{-12} \text{ cm}^3 \text{ molecule}^{-1} \text{ s}^{-1}$ at 298 K, with no measurable temperature dependence over the range 298–573. By including CO in the reaction mixture to convert OH products into readily detected CO₂ molecules, a branching ratio of <0.05 into OH producing channels was estimated. Similar experiments on the SiH₃ + O₂ reaction indicate a branching ratio of 0.076 into OH. At this point, the identity of the major product channel in these reactions is still unknown, but we have demonstrated that OH-producing channels are less important than previously believed.

Acknowledgment. This work was partially supported by the Division of Chemical Sciences, Office of Basic Energy Sciences of the Department of Energy, Grant DE-FG03-96ER14645. J.P.M. acknowledges North Dakota EPSCoR for a graduate student fellowship.

References and Notes

- (1) Pankove, J. I., Ed. *Semiconductors and Semimetals*; Academic Press: New York, 1984; Vol. 21A.
- (2) Jasinski, J. M.; Gates, S. M. *Acc. Chem. Res.* **1991**, *24*, 9.
- (3) Kushner, M. J. *J. Appl. Phys.* **1987**, *62*, 2803.
- (4) Robertson, R.; Gallagher, A. *J. Appl. Phys.* **1986**, *59*, 3402.
- (5) Gallagher, A. *J. Appl. Phys.* **1988**, *63*, 2406.
- (6) Suga, S.; Koda, S. *Jpn. J. Appl. Phys.* **1988**, *27*, L1966.
- (7) Hartman, J. R.; Famil-Ghiriha, J.; Ring, M. A.; O'Neal, H. E. *Combust. Flame* **1987**, *68*, 43.
- (8) Jasinski, J. M.; Becerra, R.; Walsh, R. *Chem. Rev.* **1995**, *95*, 1203.
- (9) Slagle, I. R.; Bernhardt, J. R.; Gutman, D. *Chem. Phys. Lett.* **1988**, *149*, 180.
- (10) Sugawara, K.; Nakanaga, T.; Takeo, H.; Matsumura, C. *Chem. Phys. Lett.* **1989**, *157*, 309.
- (11) Koshi, M.; Miyoshi, A.; Matsui, H. *J. Phys. Chem.* **1991**, *95*, 9869.
- (12) Quandt, R.; Hershberger, J. F. *Chem. Phys. Lett.* **1993**, *206*, 355.
- (13) Loh, S. K.; Beach, D. B.; Jasinski, J. M. *Chem. Phys. Lett.* **1990**, *169*, 55.
- (14) Matsumoto, K.; Koshi, M.; Okawa, K.; Matsui, H. *J. Phys. Chem.* **1996**, *100*, 8796.
- (15) Loh, S. K.; Jasinski, J. M. *J. Chem. Phys.* **1991**, *95*, 4914.
- (16) Seetula, J. A.; Feng, Y.; Gutman, D.; Seakins, P. W.; Pilling, M. J. *J. Phys. Chem.* **1991**, *95*, 1658.
- (17) Krasnoperov, L. N.; Chesnokov, E. N.; Panfilov, V. N. *Chem. Phys.* **1984**, *89*, 297.
- (18) Roland, R. P.; Bolle, M.; Anderson, R. W. *Chem. Mater.* **2001**, *13*, 2493.
- (19) Roland, R. P.; Anderson, R. W. *Chem. Mater.* **2001**, *13*, 2501.
- (20) Darling, C. L.; Schlegel, H. B. *J. Phys. Chem.* **1994**, *98*, 8910.
- (21) Koshi, M.; Nishida, N.; Murakami, Y.; Matsui, H. *J. Phys. Chem.* **1993**, *97*, 4473.
- (22) Ding, L.; Marshall, P. J. *J. Phys. Chem.* **1992**, *96*, 2197.
- (23) Niki, H.; Maker, P. D.; Savage, C. M.; Breitenbach, L. P. *J. Phys. Chem.* **1985**, *89*, 1752.
- (24) Edwards, M. A., Ph.D. Dissertation, North Dakota State University, Fargo, ND, 1998.
- (25) Sumiyoshi, Y.; Tanaka, K.; Tanaka, T. *Appl. Surf. Sci.* **1994**, *79*, 471.
- (26) Rim, K. T.; Hershberger, J. F. *J. Phys. Chem. A* **1998**, *102*, 5898.
- (27) Rothman, L. S.; Gamache, R. R.; Tipping, R. H.; Rinsland, C. P.; Smith, M. A. H.; Benner, D. C.; Devi, V. M.; Flaud, J. M.; Camy-Peyret, C.; Perrin, A.; Goldman, A.; Massie, S. T.; Brown, L. R.; Toth, R. A. *J. Quant. Spectrosc. Radiat. Transfer* **1992**, *48*, 469.
- (28) DeMore, W. B.; Sander, S. P.; Golden, D. M.; Hampson, R. F.; Kurylo, M. J.; Howard, C. J.; Ravishankara, A. R.; Kolb, C. E.; Molina, M. J. *Chemical kinetics and photochemical data for use in stratospheric modeling. Evaluation number 12*, **1997**, JPL Publication 97-4.
- (29) Cooper, W. F.; Park, J.; Hershberger, J. F. *J. Phys. Chem.* **1993**, *97*, 3283.
- (30) Jacobs, A.; Wahl, M.; Weller, R.; Wolfrum, J. *Chem. Phys. Lett.* **1988**, *144*, 203.
- (31) Atkinson, R.; Pitts, J. N., Jr. *Int. J. Chem. Kinet.* **1978**, *10*, 1151.